AD-A049 451 SCIENCE APPLICATIONS INC BERKELEY CALIF F/G 9/5
NUMERICAL RESULTS OR MULTICONDUCTOR TRANSMISSION LINE NETWORKS.(U)
NOV 77 C E BAUM, T K LIU, F M TESCHE F29601-76-C-0125
UNCLASSIFIED AFWL-TR-77-123 NL

| OF |
AD
A049 451

END
DATE
FILMED
3-78
DDC

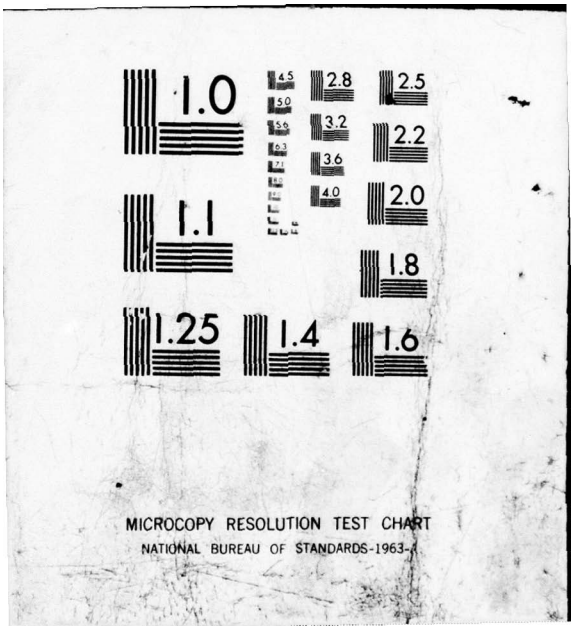
1.0
1.1
1.25
1.4
1.6
1.8
2.0
2.2
2.5
2.8
3.2
3.6
4.0
4.5
5.0
5.6
6.3
7.1
MICROCOPY RESOLUTION TEST CHART
NATIONAL BUREAU OF STANDARDS-1963-A

AFWL-TR-77-123

(2)

AFWL-TR-
77-123

NUMERICAL RESULTS OR MULTICONDUCTOR TRANSMISSION LINE NETWORKS

Science Applications, Inc.
Berkeley, CA 94701

November 1977

Final Report

Approved for public release; distribution unlimited.

AIR FORCE WEAPONS LABORATORY
Air Force Systems Command
Kirtland Air Force Base, NM 87117

This final report was prepared by Science Applications, Inc., Berkeley, CA, under Contract F29601-76-C-0125, Job Order 12090513 with the Air Force Weapons Laboratory, Kirtland Air Force Base, New Mexico. Captain Howard Hudson (ELP) is the Laboratory Project Officer-in-Charge.

When US Government drawings, specifications, or other data are used for any purpose other than a definitely related Government procurement operation, the Government thereby incurs no responsibility nor any obligation whatsoever, and the fact that the Government may have formulated, furnished, or in any way supplied the said drawings, specifications, or other data is not to be regarded by implication or otherwise as in any manner licensing the holder or any other person or corporation or conveying any rights or permission to manufacture, use, or sell any patented invention that may in any way be related thereto.

This report has been reviewed by the Officer of Information (OI) and is releasable to the National Technical Information Service (NTIS). At NTIS, it will be available to the general public, including foreign nations.

This technical report has been reviewed and is approved for publication.

HOWARD G. HUDSON,
Captain, USAF,
Project Officer

FOR THE COMMANDER

J. PHILIP CASTILLO,
Acting Chief,
Technology Branch

DONALD A. DOWLER,
Colonel, USAF,
Chief, Electromagnetics Division

DO NOT RETURN THIS COPY. RETAIN OR DESTROY.

UNCLASSIFIED

SECURITY CLASSIFICATION OF THIS PAGE (When Data Entered)

REPORT DOCUMENTATION PAGE

READ INSTRUCTIONS BEFORE COMPLETING FORM

1. REPORT NUMBER: AFWL-TR-77-123	2. GOVT ACCESSION NO.
3. RECIPIENT'S CATALOG NUMBER	
4. TITLE (and Subtitle): NUMERICAL RESULTS OR MULTICONDUCTOR TRANSMISSION LINE NETWORKS.	5. TYPE OF REPORT & PERIOD COVERED: Final Report.
	6. PERFORMING ORG. REPORT NUMBER
7. AUTHOR(s): C.E. Baum, F.M. Tesche, T.K. Liu, S.K. Chang	8. CONTRACT OR GRANT NUMBER(s): F29601-76-C-0125
9. PERFORMING ORGANIZATION NAME AND ADDRESS: Science Applications, Inc. Berkeley, California 94701	10. PROGRAM ELEMENT, PROJECT, TASK AREA & WORK UNIT NUMBERS: Program Element: 64747F JON: 1209[illegible]
11. CONTROLLING OFFICE NAME AND ADDRESS: Air Force Weapons Laboratory Kirtland Air Force Base, NM 87117	12. REPORT DATE: Nov[illegible]77
	13. NUMBER OF PAGES: 44
14. MONITORING AGENCY NAME & ADDRESS (if different from Controlling Office): Air Force Weapons Laboratory Kirtland Air Force Base, NM 87117	15. SECURITY CLASS. (of this report): Unclassified
	15a. DECLASSIFICATION/DOWNGRADING SCHEDULE

16. DISTRIBUTION STATEMENT (of this Report)

Approved for public release; distribution unlimited.

17. DISTRIBUTION STATEMENT (of the abstract entered in Block 20, if different from Report)

18. SUPPLEMENTARY NOTES

19. KEY WORDS (Continue on reverse side if necessary and identify by block number)

Electromagnetic Fields
Transmission Lines,
Multiconductor Transmission Lines
Multiconductor Transmission Line Analysis

20. ABSTRACT (Continue on reverse side if necessary and identify by block number)

This report describes the algorithms and numerical results for a lossless multiconductor transmission-line network which is excited by a number of lumped voltage and current sources located on the transmission lines. As opposed to previous analyses of multiconductor transmission lines, the method described in this report is capable of treating networks which contain one or more closed transmission-line loops. The formulation of this analysis involves defining a large matrix equation (the BLT equation for currents

DD FORM 1 JAN 73 1473 EDITION OF 1 NOV 65 IS OBSOLETE

UNCLASSIFIED

SECURITY CLASSIFICATION OF THIS PAGE (When Data Entered)

409 694

incident on each of the junctions of the transmission-line network. Matrix inversion then provides the solution for these incident currents, with the reflected current component then being determined from knowledge of the scattering properties of the junctions. The total junction currents are then found by combining the incident and reflected components. To illustrate this approach, a single-wire network and a more general multi-conductor transmission-line network are considered with numerical results for the voltages at points within the networks displayed.

TABLE OF CONTENTS

LIST OF FIGURES

SECTION I

INTRODUCTION

The use of transmission-line theory plays an important role in the analysis of system response to a nuclear electromagnetic pulse (EMP). Various transmission-line models are typically employed for EMP internal interaction studies so as to calculate how EMP energy is distributed within the interior regions of the system.

Inputs or source terms for such transmission-line models are series voltage generators and shunt current generators distributed along various portions of the transmission lines. Such sources arise from EMP energy penetrating through slits, holes, or other apertures in the outer shielding surface of the system, or diffusing through skin panels and then coupling to the transmission line.

The response of interest is usually a voltage or current at a particular point on the line, usually at an impedance element which represents the load impedance of a circuit which might be damaged or upset by the EMP transient. In many cases, both time harmonic and transient responses are considered to permit the prediction of EMP effects on the system.

One of the most straightforward approaches for solving the internal interaction problem involves modeling a complicated transmission-line network by one or more single-wire transmission lines which are interconnected in series or parallel, but with no closed loops being formed. Such single-line models are described in references (1) and (2). In addition to these, references (3) through (9) discuss

---

1. Plonsey, R., and R.E. Collin, Principles and Applications of Electromagnetic Fields, McGraw Hill, 1961.
2. Tesche, F.M., et al., Evaluation of Present Internal EMP Interaction Technology: Description of Needed Improvements, AFWL-TR-75-288, Air Force Weapons Laboratory, Kirtland Air Force Base, NM, Oct. 1973.
3. Tesche, F.M., and T.K. Liu, Selected Topics in Transmission-Line Theory for EMP Internal Interaction Problems, AFWL-TR-77-73, Air Force Weapons Laboratory, Kirtland Air Force Base, NM, Dec. 1976.

various improvements which can be made to the single-line model by more accurately accounting for the nonidealized geometry found in the actual interaction problem.

Another approach for treating the internal interaction problem is to use multiconductor transmission-line theory. While this increases the complexity of the calculations involved for a particular problem, the accuracy to which the computational model approximates the actual problem is much greater.

The anlaysis of multiconductor transmission lines is well documented in the literature. One popular approach is to employ a lumped parameter network (LPN) model for the multiconductor transmission line and then perform a circuit analysis using a large network analysis code. Such a procedure is discussed in reference (10). A major difficulty with such an approach lies in the fact that if a complicated, electrically long cable harness is to be analyzed, substantial time must be spent in defining the network to be analyzed, choosing the element values, and setting up the problem. Moreover, computation time can be substantial.

---

4. Tesche, F.M., and T.K. Liu, An Electric Model for a Cable Clamp on a Single-Wire Transmission Line, AFWL-TR-76-325, Air Force Weapons Laboratory, Kirtland Air Force Base, NM, Mar. 1977.

5. Coen, S., T.K. Liu, and F.M. Tesche, Calculation of the Equivalent Capacitance of a Rib near a Single-Wire Transmission Line, AFWL-TR-77-60, Air Force Weapons Laboratory, Kirtland Air Force Base, NM, June 1977.

6. Lee, K.S.H., and F.C. Yang, A Wire Passing by a Circular Aperture in an Infinite Ground Plane, AFWL-TR-77-52, Air Force Weapons Laboratory, Kirtland Air Force Base, NM, Feb. 1977.

7. Lam, J., Equivalent Lumped Parameters for a Bend in a Two-Wire Transmission Line, AFWL-TR-77-5, Air Force Weapons Laboratory, Kirtland Air Force Base, NM, Jan. 1977.

8. Lam, J., Propagation Characteristics of a Periodically Loaded Transmission Line, AFWL-TR-76-324, Air Force Weapons Laboratory, Kirtland Air Force Base, NM, Jan. 1977.

9. Liu, T.K., Electromagnetic Coupling between Multiconductor Transmission Lines in a Homogeneous Medium, AFWL-TR-76-333, Air Force Weapons Laboratory, Kirtland Air Force Base, NM, May 1977.

10. EMP Handbook for Missiles and Aircraft in Flight, AFWL-TR-73-68, Air Force Weapons Laboratory, Kirtland Air Force Base, NM. Also, EMP Interaction Notes, Vol. 1-1.

An alternate approach for treating the multiconductor transmission line is to solve the set of transmission-line equations directly. The solution is accomplished by using the modal concept, as discussed in references (11) through (18). This method involves determining the various quasi-TEM modes and related propagation constants which can exist on the multiconductor transmission line. This is achieved by determining the eigenvalues and eigenvectors of a propagation matrix which contains the fundamental line parameters. The total solution for voltage or current on the multiconductor line is then describable as a linear combination of all possible modes on the line.

Previous application of multiconductor transmission-line theory to the internal interaction problem has involved simple branching transmission lines or, at times, a single section of line. To solve the transmission-line network problem with branching, all branches except one are represented by a Thévenin or Norton equivalent circuit and the

---

11. Carson, J.R., "The Rigorous and Approximate Theories of Electrical Transmission along Wires," Bell System Technical Journal, No. 1, Jan. 1928, pp. 11-23.

12. Kuznetsov, P.I., and R.L. Stratonovich, The Propagation of Electromagnetic Waves in Multiconductor Transmission Lines, Pergamon Press, Oxford, England, 1964.

13. Kajfez, D., "Multiconductor Transmission Lines," AFWL EMP Interaction Notes, Note 151, June 1972.

14. Paul, C.R., "On Uniform Multimode Transmission Lines," IEEE Trans. M.T.T., Vol. MTT-21, No. 8, Aug. 1973, pp. 556-558.

15. Paul, C.R., "Efficient Numerical Computation of the Frequency Response of Cables Illuminated by an Electromagnetic Field," IEEE Trans. M.T.T., Vol. MTT-52, No. 4, Apr. 1974, pp. 454-457.

16. Paul, C.R., "Useful Matrix Chain Parameter Identities for the Analysis of Multiconductor Transmission Lines," IEEE Trans. M.T.T., Sept. 1975, pp. 756-760.

17. Frankel, S., Cable and Multiconductor Transmission Analysis, Harry Diamond Laboratory, HDL-TR-091-1, June 1974.

18. Lenahan, T.A., "The Theory of Uniform Cables, Parts I & II," Bell System Technical Journal, April 1977, pp. 597-625.

resulting single-section transmission line is solved to obtain voltages and currents. This process is repeated until all branches in the network are all studied. Not only is this method tedious and time consuming, but it has the weakness of not being able to treat transmission-line networks with complicated branching or connections involving closed loops.

In many practical cases, however, the wiring configuration is not simple. In general, there may be a variety of closed loops formed by transmission lines in an actual system, and induced currents on this transmission-line network can behave quite differently from currents induced on a simple branching transmission-line network.

The method adopted in this report of analyzing a general lossless multiconductor transmission-line network is based on the scattering matrix technique used widely in distributed network analysis (ref. 19). Thus, at a junction where a number of transmission-line tubes meet, the reflected currents (or voltages) at the nodes are related by a scattering matrix to the incident currents (or voltages) at all the nodes at the same junction. These quantities at the two ends of a branch are also related by a propagation matrix. With the knowledge of excitation sources and termination conditions, these two relations are sufficient to yield the current (and voltage) at all nodes by means of matrix inversion. This procedure is similar to the solution of lumped circuit problems using mesh analysis (ref. 20), and has been discussed recently in the literature (refs. 21 through 23).

---

19. Collin, R.E., Foundations for Microwave Engineering, McGraw Hill, New York, 1966.

20. Desoer, C.A., and E.S. Kuh, Basic Circuit Theory, McGraw Hill, New York, 1969.

21. Baum, C.E., "The Role of Scattering Theory in Electromagnetic Interference Problems," in Electromagnetic Scattering, P.L.E. Uslenghi (ed.), to be published.

22. Baum, C.E., "Coupling into Coaxial Cables from Currents and Charges on the Exterior," presented at the 1976 URSI Meeting, Amherst, Mass.

23. Tesche, F.M., "A General Multiconductor Transmission-Line Model." presented at the 1976 URSI Meeting, Amherst, Mass.

This report is intended to give a concise summary of the solution procedures for lossless multiconductor transmission-line networks. The detail description of the basic theory is discussed in a separate report (ref. 24). Reference (24) also treats the more general transmission-line networks that may include losses.

Various definitions and concepts are introduced in Section II. The overall procedure of solving the transmission-line network problem is also summarized. In Section III, an example of how to apply this method, as well as some numerical results, are given.

---

24. Baum, C.E., T.K. Liu and F.M. Tesche, "On the General Analysis of Multiconductor Transmission-Line Networks," AFWL EMP Interaction Notes, to be published.

SECTION II

BASIC CONCEPTS AND APPROACH

In this section, a few definitions and concepts that are unique to general transmission-line networks are first introduced. These quantities are useful for the discussions in the later part of this section and the rest of the report. Detailed descriptions of these quantities are presented in reference (24). The fundamental relations needed for the development of the computer code are then summarized.

1. Graph Representation

In Figure 1a, a simple multiconductor transmission-line network is shown. In analogy to the lumped network analysis, a graph is introduced in Figure 1b to represent the entire network. The basic elements of the graph are tubes and junctions. A tube is a section of multiconductor transmission line with uniform or gradually changing configurations. In this report, we assume that there is one common reference conductor for the whole network.

A junction is where one or more tubes meet. We denote a junction by J_j, $j=1,2,\ldots,N_J$, where N_J is the total number of junctions within the entire network. A tube connected between junctions J_j and J_k is denoted by $T_{j,k}$. Thus, $T_{j,k}$ identifies the same tube as $T_{k,j}$, assuming there is only one tube between the two junctions.

The network graph representation enables one to visualize the overall network connections in a simple form and is particularly useful when the network is extremely complicated and contains a number of closed loops and crossed connections. Here, a double line represents a tube which contains many conductors and is a distributed element, and a circle represents a junction within which multiple connections between conductors of the tubes are possible.

Figure 1b does not completely describe the network topology. Details of intertube connections within a junction must be described.

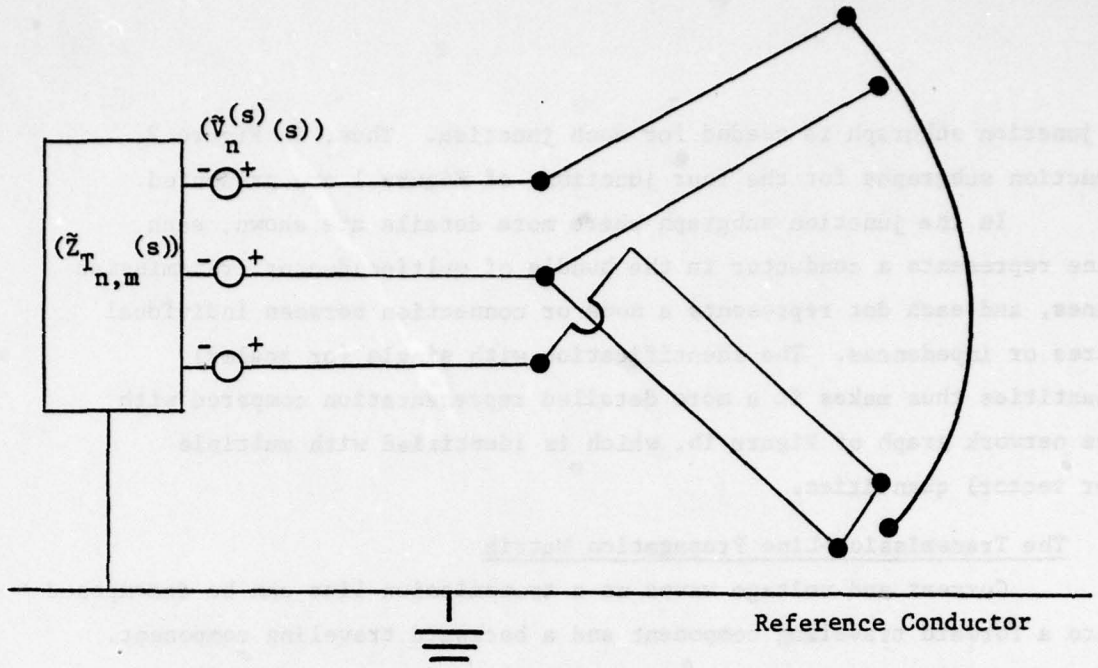

(a)

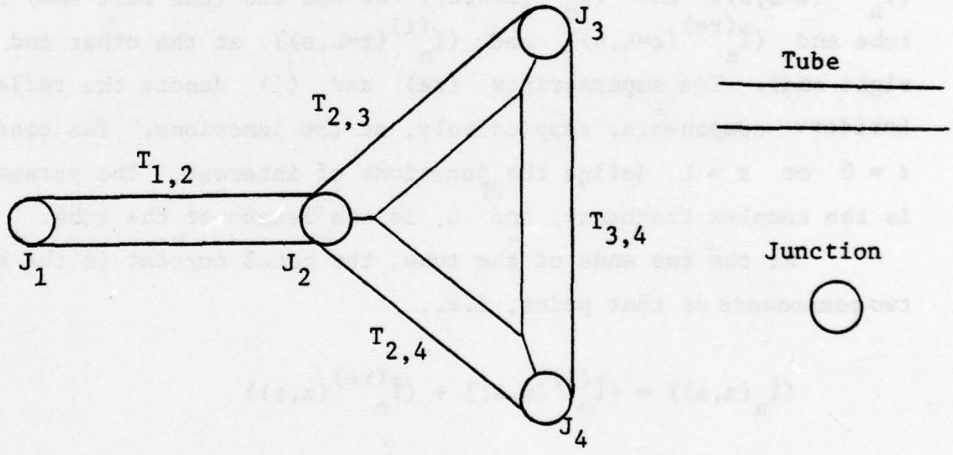

(b)

Figure 1. (a) A simple mutliconductor transmission-line network, and
(b) its associated graph.

A junction subgraph is needed for each junction. Thus, in Figure 2, junction subgraphs for the four junctions of Figure 1 are presented.

In the junction subgraph where more details are shown, each line represents a conductor in the bundle of multiconductor transmission lines, and each dot represents a node or connection between individual wires or impedances. The identification with single (or scalar) quantities thus makes it a more detailed representation compared with the network graph of Figure 1b, which is identified with multiple (or vector) quantities.

2. The Transmission-Line Propagation Matrix

Current and voltage waves on a transmission line can be decomposed into a forward traveling component and a backward traveling component. At a junction, these components are also identified as the incident and reflected components. Let us consider a typical single tube (see Figure 3) which is spanned between two junctions with voltage and current sources at $z = \xi$. Here we denote the two components by $(\tilde{I}_n^{(re)}(z=0,s))$ and $(\tilde{I}_n^{(i)}(z=0,s))$ at one end (the left end) of the tube and $(\tilde{I}_n^{(re)}(z=L,s))$ and $(\tilde{I}_n^{(i)}(z=L,s))$ at the other end (the right end). The superscripts (re) and (i) denote the reflected and incident components, respectively, at the junctions. The conditions $z = 0$ or $z = L$ define the junctions of interest. The parameter s is the complex frequency, and L is the length of the tube.

At the two ends of the tube, the total current is the sum of the two components at that point, i.e.,

$$(\tilde{I}_n(z,s)) = (\tilde{I}_n^{(i)}(z,s)) + (\tilde{I}_n^{(re)}(z,s)) \qquad (1)$$

where $z = 0$ or $z = L$.

For a tube of multiconductor transmission line with N_c conductors plus a reference, there are N_c propagating modes (refs. 3 and 14). In relating currents at different positions along the tube, it is necessary to (i) decompose the total current into modal currents,

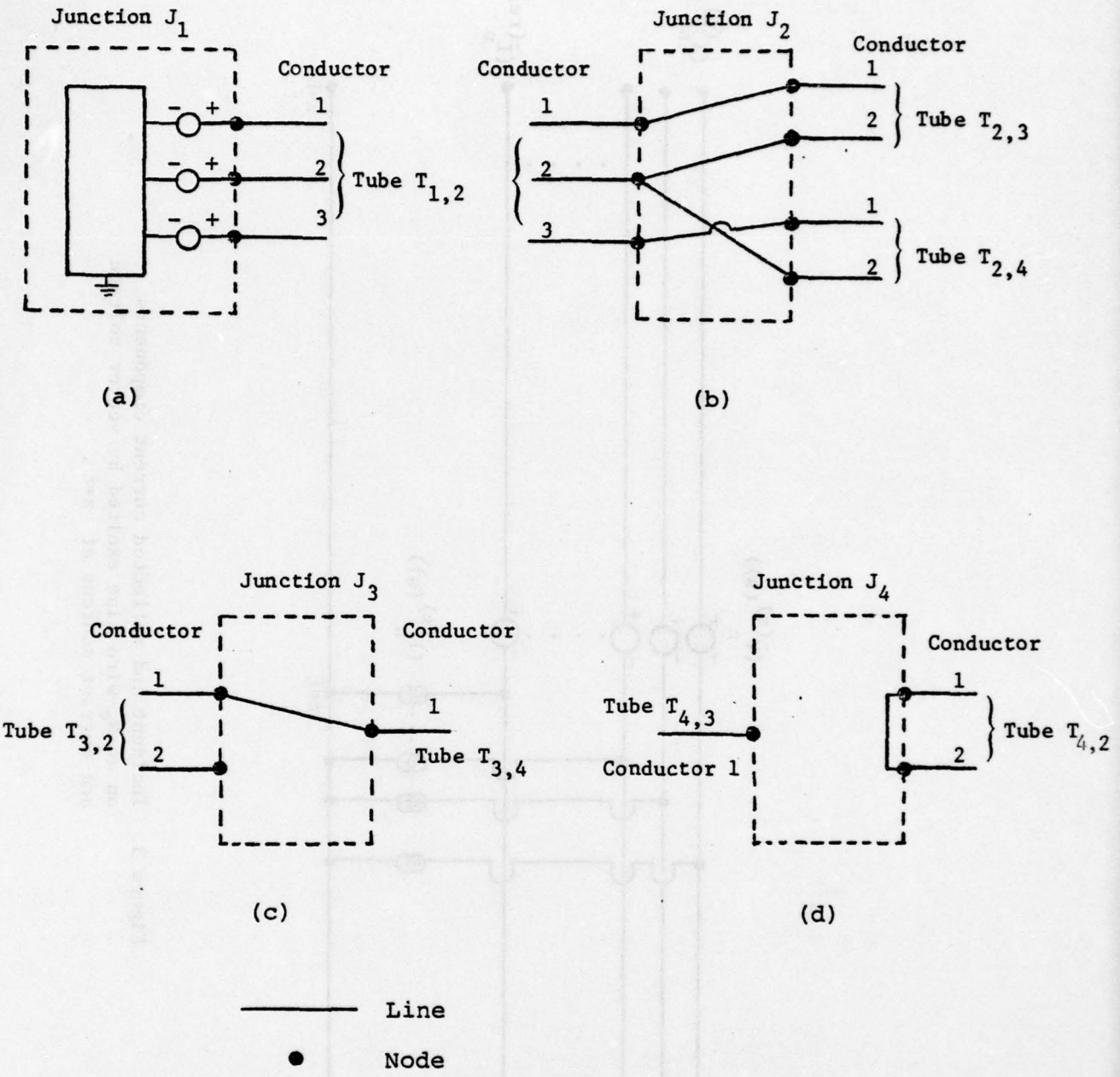

Figure 2. Junction subgraph at junction (a) 1, (b) 2, (c) 3, (d) 4.

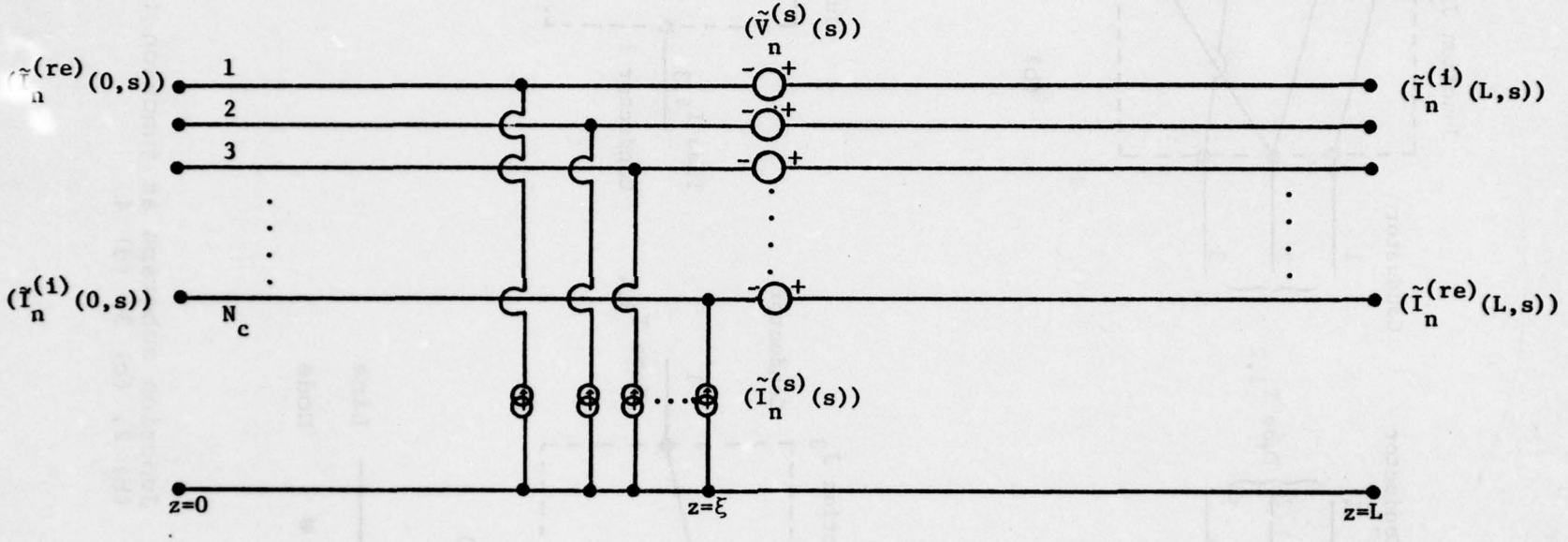

Figure 3. Incident and reflected current components on an N_c-wire line excited by vector voltage and current sources at $z=\xi$.

(ii) relate the modal currents at different positions by the modal propagation matrix, and (iii) convert the modal components so related back to the total current.

Details of this procedure have been described in references (3) and (24). Here, we summarize the important results in the following.

For the lossless case, the modal current $(\tilde{I}_{c_n}(s))$ is defined so that

$$(\tilde{I}_n(z,s)) = (\mathcal{J}_{n,m})\cdot(\tilde{I}_{c_n}(s)) \tag{2}$$

where $(\mathcal{J}_{n,m})$ is the similarity transform matrix formed by the eigenvectors of the matrix $((C'_{n,m})\cdot(L'_{n,m}))$. The corresponding eigenvalues of $(\mathcal{J}_{n,m})$ are the elements of the diagonal matrix $(\tilde{\gamma}_{c_{n,m}}(s))^2$, which is given by

$$(\tilde{\gamma}_{c_{n,m}}(s))^2 = s^2(\mathcal{J}_{n,m})^{-1}\cdot(C'_{n,m})\cdot(L'_{n,m})\cdot(\mathcal{J}_{n,m}) \tag{3}$$

The elements of $(\tilde{\gamma}_{c_{n,m}}(s))$ are in the form of s/(mode velocity). The characteristic impedance matrix $(Z_{c_{n,m}})$ is given by

$$(Z_{c_{n,m}}) = (C'_{n,m})^{-1}\cdot(\mathcal{J}_{n,m})\cdot(\tilde{\gamma}_{c_{n,m}}(s))\cdot(\mathcal{J}_{n,m})^{-1}/s \tag{4}$$

The reflected current components at the two ends of the tube are related to the incident components by

$$\begin{pmatrix}(\tilde{I}_n^{(re)}(0,s))\\(\tilde{I}_n^{(re)}(L,s))\end{pmatrix} = \begin{pmatrix}(0_{n,m}) & (\tilde{P}_{n,m}(s))\\(\tilde{P}_{n,m}(s)) & (0_{n,m})\end{pmatrix}\cdot\begin{pmatrix}(\tilde{I}_n^{(i)}(0,s))\\(\tilde{I}_n^{(i)}(L,s))\end{pmatrix} + (\tilde{\mathcal{P}}_n^{(s)}(s)) \tag{5}$$

where $(\tilde{P}_{n,m}(s))$ is the current propagation matrix of the tube and is given by

$$(\tilde{P}_{n,m}(s)) = (\mathcal{J}_{n,m}) \cdot (\exp(\tilde{\gamma}_{c_{n,m}}(s))L) \cdot (\mathcal{J}_{n,m})^{-1} \qquad (6)$$

$(\tilde{\mathcal{G}}_n^{(s)}(s))$ is the source vector of the tube referred to the two ends, and is given by

$$(\tilde{\mathcal{G}}_n^{(s)}(s)) = \begin{pmatrix} -\frac{1}{2}(\mathcal{J}_{n,m}) \cdot (\exp(\tilde{\gamma}_{c_{n,m}}(s))\xi) \cdot (\mathcal{J}_{n,m})^{-1} \\ \\ \frac{1}{2}(\mathcal{J}_{n,m}) \cdot (\exp(\tilde{\gamma}_{c_{n,m}}(s))[L-\xi]) \cdot (\mathcal{J}_{n,m})^{-1} \end{pmatrix}$$

$$\begin{pmatrix} \cdot[(\tilde{I}_n^{(s)}(\xi,s)) + (Z_{c_{n,m}})^{-1} \cdot (\tilde{V}_n^{(s)}(\xi,s))] \\ \\ \cdot[(\tilde{I}_n^{(s)}(\xi,s)) - (Z_{c_{n,m}})^{-1} \cdot (\tilde{V}_n^{(s)}(\xi,s))] \end{pmatrix} \qquad (7)$$

If the tube is excited by distributed voltage source $(V_n^{(s)'}(z,s))$ and distributed current source $(I_n^{(s)'}(z,s))$, then

$$(\tilde{\mathcal{G}}_n^{(s)}(s)) = \int_0^L \begin{pmatrix} -\frac{1}{2}(\mathcal{J}_{n,m}) \cdot (\exp(\tilde{\gamma}_{c_{n,m}}(s))\xi) \cdot (\mathcal{J}_{n,m})^{-1} \\ \\ \frac{1}{2}(\mathcal{J}_{n,m}) \cdot (\exp(\tilde{\gamma}_{c_{n,m}}(s))[L-\xi]) \cdot (\mathcal{J}_{n,m})^{-1} \end{pmatrix}$$

$$\begin{pmatrix} \cdot[(\tilde{I}_n^{(s)'}(\xi,s)) + (Z_{c_{n,m}}(s))^{-1} \cdot (\tilde{V}_n^{(s)'}(\xi,s))] \\ \\ \cdot[(I_n^{(s)'}(\xi,s)) - (Z_{c_{n,m}}(s))^{-1} \cdot (\tilde{V}_n^{(s)'}(\xi,s))] \end{pmatrix} d\xi$$

For the tube with N_c conductors (plus a reference), $(\tilde{P}_{n,m}(s))$ is an $N_c \times N_c$ matrix and $(\tilde{\mathcal{G}}_n^{(s)}(s))$ is a $2N_c \times 1$ vector.

At the two ends of the tube the total voltage is given by

$$(\tilde{V}_n(z,s)) = q(Z_{c_{n,m}})\cdot((\tilde{I}_n^{(re)}(z,s)) - (\tilde{I}_n^{(i)}(z,s))) \qquad (8)$$

where $q = +1$ at $z = 0$ and $q = -1$ at $z = L$.

3. The Junction Scattering Matrix

For a junction J_j with N_{J_j} tubes connected, the quantities associated with tube T_{j,k_i} are denoted by the subscript T_{j,k_i}, $i = 1,2,\ldots,N_{J_j}$. For example, $(\tilde{I}_n(z,s))_{T_{j,k_i}}$ is the current vector of Tube T_{j,k_i}.

For distributed circuits, the reflected and incident quantities at a junction are often related by a scattering matrix (ref. 19). For junction J_j the current junction scattering matrix $(\tilde{S}_{n,m}(s))_{J_j}$ is defined so that

$$\begin{pmatrix} (\tilde{I}_n^{(re)}(z_{j,k_1},s))_{T_{j,k_1}} \\ (\tilde{I}_n^{(re)}(z_{j,k_2},s))_{T_{j,k_2}} \\ \vdots \\ (\tilde{I}_n^{(re)}(z_{j,k_{N_{J_j}}},s))_{T_{j,k_{N_{J_j}}}} \end{pmatrix} = (\tilde{S}_{n,m}(s))_{J_j} \cdot \begin{pmatrix} (\tilde{I}_n^{(i)}(z_{j,k_1},s))_{T_{j,k_1}} \\ (\tilde{I}_n^{(i)}(z_{j,k_2},s))_{T_{j,k_2}} \\ \vdots \\ (\tilde{I}_n^{(i)}(z_{j,k_{N_{J_j}}},s))_{T_{j,k_{N_{J_j}}}} \end{pmatrix} \qquad (9)$$

where z_{j,k_i}, $i = 1,2,\ldots N_{J_j}$ is taken to be the appropriate coordinate of the tube T_{j,k_i} at the j junction J_j.

From Equation (9), it is clear that the submatrix $(\tilde{S}_{n,m})_{J_j}$ is given by

$$(\tilde{I}_n^{(re)}(z_{j,k_n},s)) = (\tilde{S}_{n,m}(s))_{J_j}\cdot(\tilde{I}^{(i)}(z_{j,k_m}s))$$

Thus, for $n = m$, $(\tilde{S}_{n,m})_{J_j}$ is the current reflection matrix, whereas for $n \neq m$, $(\tilde{S}_{n,m})_{J_j}$ is the transmission matrix.

Two cases of particular interest are treated here: (i) junctions contain tubes only which are interconnected, and (ii) junctions where a tube is terminated by external impedances.

(a) Junctions with tubes only

At a junction where there are only direct connections between tubes, the Kirchhoff current law and the Kirchhoff voltage law have to be enforced.

Kirchhoff's current law states that the sum of the current flowing <u>out</u> a node is zero. For the case that the n_1-th wire of tube T_{j,k_1} is connected to the n_2-th wire of tube T_{j,k_2}, and to the $n_{N_{J_j}}$-th wire of tube $T_{j,k_{N_{J_j}}}$, etc., then

$$q_{j,k_1} \tilde{I}_{n_1}(z_{j,k_1}, s)\Big|_{T_{j,k_1}} + q_{j,k_2} \tilde{I}_{n_2}(z_{j,k_2}, s)\Big|_{T_{j,k_2}} + \ldots + q_{j,k_{N_{J_j}}} \tilde{I}_{n_{N_{J_j}}}(z_{j,k_{N_{J_j}}}, s)\Big|_{T_{j,k_{N_{J_j}}}} = 0 \qquad (10)$$

where $q_{j,k_i} = +1$ if $z_{j,k_i} = 0$ and $q_{j,k_i} = -1$ if $z_{j,k_i} = L_{j,k_i}$, $i = 1, 2, \ldots, N_{J_j}$.

Equation (10) can be put into the matrix form, i.e.,

$$\overbrace{(0\ 0\ \ldots\ q_{j,k_1}\ \ldots\ 0}^{T_{j,k_1}}\ \overbrace{0\ \ldots\ q_{j,k_2}\ \ldots 0}^{T_{j,k_2}}\ \ldots\ \overbrace{0\ \ldots\ q_{j,k_{N_{J_j}}}\ \ldots\ 0)}^{T_{j,k_{N_{J_j}}}}$$

$$\cdot \begin{pmatrix} (\tilde{I}_n(z_{j,k_1},s))_{T_{j,k_1}} \\ (\tilde{I}_n(z_{j,k_2},s))_{T_{j,k_2}} \\ \vdots \\ (\tilde{I}_n(z_{j,k_{N_{J_j}}},s))_{T_{j,k_{N_{J_j}}}} \end{pmatrix} = (0_n) \qquad (11)$$

In Equation (11), all elements in the left matrix are zero unless they correspond to the conductors which are connected at the node. For K_{J_j} connections within the junction J_j, there are K_{J_j} equations similar to Equation (10), and we can define the junction connection matrix $(C_{I_{n,m}})_{J_j}$ so that

$$(C_{I_{n,m}})_{J_j} \cdot \begin{pmatrix} (\tilde{I}_n(z_{j,k_1},s))_{T_{j,k_1}} \\ (\tilde{I}_n(z_{j,k_2},s))_{T_{j,k_2}} \\ \vdots \\ (\tilde{I}_n(z_{j,k_{N_{J_j}}},s))_{T_{j,k_{N_{J_j}}}} \end{pmatrix} = (0_{n,m}) \qquad (12)$$

where $(C_{I_{n,m}})_{J_j}$ is a $K_{J_j} \times M_{J_j}$ matrix, and M_{J_j} is the total number of conductors connected to junction J_j, i.e.,

$$M_{J_j} = \sum_{i=1}^{N_{J_j}} N_c\Big|_{T_{j,k_i}}$$

where $N_c\Big|_{T_{j,k_i}}$ is the number of conductors of tube T_{j,k_i}.

Kirchhoff's voltage law, for the case of simple connections, requires all voltages associated with each conductor to be the same at the same node. Thus, in the particular example above, we have

$$\tilde{V}_{n_1}(z_{j,k_1},s)\Big|_{T_{j,k_1}} - \tilde{V}_{n_2}(z_{j,k_2},s)\Big|_{T_{j,k_2}} = 0$$

$$\tilde{V}_{n_2}(z_{j,k_2},s)\Big|_{T_{j,k_2}} - \cdots\cdots = 0$$

$$\cdots\cdots$$

$$\cdots\cdots - \tilde{V}_{n_{N_{J_j}}}(z_{j,k_{N_{J_j}}},s)\Big|_{T_{j,k_{N_{J_j}}}} = 0$$

The above equation can be easily written in matrix form. For a consistent set of connections, there are $M_{J_j} - K_{J_j}$ equations. Let us denote the corresponding matrix as $(C_{V_{n,m}})_{J_j}$ such that

$$(C_{V_{n,m}})_{J_j} \cdot \begin{pmatrix} (\tilde{V}_n(z_{j,k_1},s))_{T_{j,k_1}} \\ (\tilde{V}_n(z_{j,k_2},s))_{T_{j,k_2}} \\ \vdots \\ (\tilde{V}_n(z_{j,k_{N_{J_j}}},s))_{T_{j,k_{N_{J_j}}}} \end{pmatrix} = (0_{n,m}) \qquad (13)$$

In addition to the above, two special situations have to be considered: (i) a conductor is open-circuited, and (ii) a conductor is short-circuited to ground.

When the n_i-th conductor of tube T_{j,k_i} is open-circuited, the current there is zero and we have

$$\tilde{I}_{n_i}(z_{j,k_i},s)\Big|_{T_{j,k_i}} = 0 \tag{14}$$

This corresponds to the entry of the value 1 at the appropriate location in the matrix $(C_{I_{n,m}})_{J_j}$ in a row where all other elements are zero. In this case, there is no corresponding equation for the voltage law.

When a conductor is short-circuited to ground, the voltage at the node is zero, i.e.,

$$\tilde{V}_{n_i}(z_{j,k_i},s)\Big|_{T_{j,k_i}} = 0 \tag{15}$$

This corresponds to a value of 1 for the appropriate element in the matrix $(C_{V_{n,m}})_{J_j}$ in a row where all other elements are zero.

Using Equations (1), (8), (12) and (13), the current scattering matrix is given by

$$(\tilde{S}_{n,m}(s))_{J_j} = \begin{pmatrix} -(C_{I_{n,m}})_{J_j} \\ (C_{V_{n,m}})_{J_j} \cdot (q_{j,k}(Z_{c_{n,m}}))_{T_{j,k}} \end{pmatrix}^{-1} \cdot \begin{pmatrix} (C_{I_{n,m}})_{J_j} \\ (C_{V_{n,m}})_{J_j} \cdot (q_{j,k}(Z_{c_{n,m}}))_{T_{j,k}} \end{pmatrix} \tag{16}$$

(b) Junctions with termination impedance

For a tube terminated in an impedance network $(\tilde{Z}_{T_{n,m}}(s))$, the current scattering matrix $(\tilde{S}_{n,m}(s))$ relates the reflected and incident current components of the tube, i.e,

$$\tilde{I}_n^{(re)}(z,s) = (\tilde{S}_{n,m}(s)) \cdot (\tilde{I}_n^{(i)}(z,s)) \tag{17}$$

In this case, $(\tilde{S}_{n,m}(s))$ is identical to the current reflection matrix $(\tilde{\Gamma}_{n,m}(s))$, which is given by (ref. 3)

$$(\tilde{S}_{n,m}(s)) = (\tilde{\Gamma}_{n,m}(s)) = -((\tilde{Z}_{T_{n,m}}(s)) + (Z_{c_{n,m}}))^{-1} \cdot ((\tilde{Z}_{T_{n,m}}(s)) - (Z_{c_{n,m}})) \tag{18}$$

4. Solution of the Network Problem--The BLT Equation

After evaluating the current propagation matrices $(\tilde{P}_{n,m}(s))$ and the source vectors $(\tilde{\mathcal{J}}_n^{(s)}(s))$ for all tubes, and the current scattering matrices $(\tilde{S}_{n,m}(s))_{J_i}$ for all junctions, one can combine these quantities and obtain a network equation, which has been called the BLT equation.

Each of these above matrices or vector must be arranged to fit into the overall network matrices or vectors. This re-arrangement can be achieved by either a matrix transformation (ref. 23) or by carefully renumbering the individual matrix and vector elements to fit into the network matrices and vectors. Another way is to consider the network quantities as supermatrices or tensors of rank four (ref. 24).

For the network, we have

$$(\tilde{I}_n^{(re)}(s))_N = (\tilde{S}_{n,m}(s))_N \cdot (\tilde{I}_n^{(i)}(s))_N \tag{19}$$

and

$$(\tilde{I}_n^{(re)}(s))_N = (\tilde{P}_{n,m}(s))_N \cdot (\tilde{I}_n^{(i)}(s))_N + (\tilde{\mathcal{V}}_n^{(s)}(s))_N \qquad (20)$$

where all matrices with subscript N indicate network quantities. Note that here the network current vectors are defined by referring to the tube numbers. An alternate way is to refer to the wavenumbers as discussed in reference (24).

Combining Equations (19) and (20), we obtain one form of the BLT equation, viz.

$$((\tilde{S}_{n,m}(s))_N - (\tilde{P}_{n,m}(s))_N) \cdot (\tilde{I}_n^{(i)}(s))_N = (\tilde{\mathcal{V}}_n^{(s)}(s))_N \qquad (21)$$

The total current is obtained by combining Equations (1) and (21)

$$(\tilde{I}_n(s))_N = ((\tilde{I}_{n,m}) + (\tilde{S}_{n,m}(s))_N) \cdot ((1_{n,m}) - (\tilde{P}_{n,m})_N)^{-1} \cdot (\tilde{\mathcal{V}}_n^{(s)}(s))_N \qquad (22)$$

where $(1_{n,m})$ is the indentity matrix, defined by

$$1_{n,m} = \begin{cases} 1 & \text{for } n = m \\ 0 & \text{for } n \neq m \end{cases}$$

= Kronecker delta

SECTION III

EXAMPLES

In this section, an example of a multiconductor transmission-line network is first presented. Numerical results for a single transmission-line network and a more general multiconductor network are then given.

1. Example for a Multiconductor Transmission-Line Network

Consider the multiconductor transmission-line network of Figure 1a. Let us label the tubes and junctions as in the graph of Figure 1b. The junction subgraphs are illustrated in Figure 2. In this example, we first demonstrate how to obtain the matrices $(\tilde{P}_{n,m}(s))_N$, $(\tilde{S}_{n,m}(s))_N$ and $(\tilde{\mathcal{J}}_n^{(s)}(s))_N$.

(a) The propagation matrix

For tube $T_{1,2}$ the current propagation matrix $(\tilde{P}_{n,m}(s))_{T_{1,2}}$ is given by Equation (6) with $(\tilde{\gamma}_{c_{n,m}}(s))^2_{T_{1,2}}$ given by Equation (3). The tube source vector $(\tilde{\mathcal{J}}_n^{(s)}(s))^{n,m}_{T_{1,2}}$ is given by Equation (7), i.e.,

$$(\tilde{\mathcal{J}}_n^{(s)}(s))_{T_{1,2}} = \begin{pmatrix} -\frac{1}{2}(\tilde{Z}_{c_{n,m}}(s))^{-1}_{T_{1,2}} \cdot (\tilde{V}_n^{(s)}(0,s))_{T_{1,2}} \\ -\frac{1}{2}(\mathcal{J}_{n,m})_{T_{1,2}} \cdot (\exp(\tilde{\gamma}_{c_{n,m}}(s))_{T_{1,2}} L_{1,2}) \cdot \\ \qquad (\mathcal{J}_{n,m})^{-1}_{T_{1,2}} \cdot (\tilde{Z}_{c_{n,m}}(s))^{-1}_{T_{1,2}} \cdot (\tilde{V}_n^{(s)}(0,s))_{T_{1,2}} \end{pmatrix}$$

where $(\mathcal{J}_{n,m})_{T_{1,2}}$ is formed by the eigenvectors of the matrix $(C'_{n,m})_{T_{1,2}} \cdot (L'_{n,m})_{T_{1,2}}$.

For Tube $T_{2,3}$, we have $(\tilde{P}_{n,m}(s))_{T_{2,3}}$ and $(\tilde{\gamma}_{c_{n,m}}(s))_{T_{2,3}}$ given by, respectively, Equations (6) and (3), and there is no source vector.

Similar procedures are applied to tubes $T_{3,4}$ and $T_{2,4}$.

The network propagation matrix $(\tilde{P}_{n,m}(s))_N$ and the network source vector can be readily identified using the results above, and we have

$$
\begin{bmatrix}
(\tilde{I}_n^{(re)}(0,s))_{T_{1,2}} \\
(\tilde{I}_n^{(re)}(L_{1,2},s))_{T_{1,2}} \\
(\tilde{I}_n^{(re)}(0,s))_{T_{2,3}} \\
(\tilde{I}_n^{(re)}(L_{2,3},s))_{T_{2,3}} \\
(\tilde{I}_n^{(re)}(0,s))_{T_{2,4}} \\
(\tilde{I}_n^{(re)}(L_{2,4},s))_{T_{2,4}} \\
(\tilde{I}_n^{(re)}(0,s))_{T_{3,4}} \\
(\tilde{I}_n^{(re)}(L_{3,4},s))_{T_{3,4}}
\end{bmatrix}
=
\begin{bmatrix}
(0_{n,m}) & (\tilde{P}_{n,m}(s))_{T_{1,2}} & & & \\
(\tilde{P}_{n,m}(s))_{T_{1,2}} & (0_{n,m}) & & (0_{n,m}) & \\
 & & (0_{n,m}) & (\tilde{P}_{n,m}(s))_{T_{2,3}} & \\
 & & (\tilde{P}_{n,m}(s))_{T_{2,3}} & (0_{n,m}) & \\
 & & & & (0_{n,m}) \quad (\tilde{P}_{n,m}(s))_{T_{2,4}} \\
 & (0_{n,m}) & & & (\tilde{P}_{n,m}(s))_{T_{2,4}} \quad (0_{n,m}) \\
 & & & & (0_{n,m}) \quad (\tilde{P}_{n,m}(s))_{T_{3,4}} \\
 & & & & (\tilde{P}_{n,m}(s))_{T_{3,4}} \quad (0_{n,m})
\end{bmatrix}
\cdot
\begin{bmatrix}
(\tilde{I}_n^{(i)}(0,s))_{T_{1,2}} \\
(\tilde{I}_n^{(i)}(L_{1,2},s))_{T_{1,2}} \\
(\tilde{I}_n^{(i)}(0,s))_{T_{2,3}} \\
(\tilde{I}_n^{(i)}(L_{2,3},s))_{T_{2,3}} \\
(\tilde{I}_n^{(i)}(0,s))_{T_{2,4}} \\
(\tilde{I}_n^{(i)}(L_{2,4},s))_{T_{2,4}} \\
(\tilde{I}_n^{(i)}(0,s))_{T_{3,4}} \\
(\tilde{I}_n^{(i)}(L_{3,4},s))_{T_{3,4}}
\end{bmatrix}
$$

$$
+
\begin{bmatrix}
(\tilde{\rho}_n^{(s)}(s))_{T_{1,2}} \\
(0_n) \\
(0_n) \\
(0_n) \\
(0_n) \\
(0_n) \\
(0_n)
\end{bmatrix}
\qquad (23)
$$

(b) The scattering matrix

For junction J_1 where tube $T_{1,2}$ is terminated in the impedance $(\tilde{Z}_{T_{n,m}}(s))_{J_1}$ by Equation (18)

$$(\tilde{S}_{n,m}(s))_{J_1} = -((\tilde{Z}_{T_{n,m}}(s))_{J_1} - (Z_{c_{n,m}})_{T_{1,2}})^{-1} \cdot ((Z_{T_{n,m}}(s))_{J_1} - (Z_{c_{n,m}})_{T_{1,2}})$$

For junction J_2, the junction connection matrix is

$$(C_{I_{n,m}})_{J_2} = \begin{array}{c} \begin{matrix} \text{Tube } T_{1,2} & & & \text{Tube } T_{2,3} & & \text{Tube } T_{2,4} & \\ \end{matrix} \\ \left[\begin{array}{ccc|cc|cc} 1 & 0 & 0 & -1 & 0 & 0 & 0 \\ 0 & 1 & 0 & 0 & -1 & 0 & -1 \\ 0 & 0 & 1 & 0 & 0 & -1 & 0 \end{array}\right] \end{array}$$

The corresponding C_V is

$$(C_{V_{n,m}})_{J_2} = \begin{array}{c} \begin{matrix} \text{Tube } T_{1,2} & & & \text{Tube } T_{2,3} & & \text{Tube } T_{2,4} & \\ \end{matrix} \\ \left[\begin{array}{ccc|cc|cc} 1 & 0 & 0 & -1 & 0 & 0 & 0 \\ 0 & 1 & 0 & 0 & -1 & 0 & 0 \\ 0 & 0 & 0 & 0 & 1 & 0 & -1 \\ 0 & 0 & 1 & 0 & 0 & -1 & 0 \end{array}\right] \end{array}$$

The matrix of all characteristic impedances at junction J_2 is thus

$$(q_{n,m}(Z_{c_{n,m}}(s))_{J_2} = \begin{bmatrix} -(Z_{c_{n,m}})_{T_{2,1}} & (0_{n,m}) & (0_{n,m}) \\ (0_{n,m}) & (Z_{c_{n,m}})_{T_{2,3}} & (0_{n,m}) \\ (0_{n,m}) & (0_{n,m}) & (Z_{c_{n,m}})_{T_{2,4}} \end{bmatrix}$$

The scattering matrix is thus given by Equation (16). Hence, collecting terms, we have

$$\begin{pmatrix} (\tilde{I}_n^{(re)}(L_{2,1}s))_{T_{2,1}} \\ (\tilde{I}_n^{(re)}(0,s))_{T_{2,3}} \\ (\tilde{I}_n^{(re)}(0,s))_{T_{2,4}} \end{pmatrix} = \begin{pmatrix} (\zeta_{n,m})_1 & (\zeta_{n,m})_2 & (\zeta_{n,m})_3 \\ (\zeta_{n,m})_4 & (\zeta_{n,m})_5 & (\zeta_{n,m})_6 \\ (\zeta_{n,m})_7 & (\zeta_{n,m})_8 & (\zeta_{n,m})_9 \end{pmatrix} \begin{pmatrix} (\tilde{I}_n^{(i)}(L_{2,1}s))_{T_{2,1}} \\ (\tilde{I}_n^{(i)}(0,s))_{T_{2,3}} \\ (\tilde{I}_n^{(i)}(0,s))_{T_{2,4}} \end{pmatrix}$$

where $(\tilde{S}_{n,m}(s))_{J_2}$ is rewritten to contain the submatrices $(\zeta_{n,m})$. The use of the submatrices $(\zeta_{n,m})$ are useful to visualize when filling up the network scattering matrix $(\tilde{S}_{n,m}(s))_N$.

For junction J_3, we have

$$(C_{I_{n,m}})_{J_3} = \left[\begin{array}{cc|c} \multicolumn{2}{c|}{\text{Tube } T_{3,2}} & \text{Tube } T_{3,4} \\ \hline 1 & 0 & -1 \\ 0 & 1 & 0 \end{array}\right]$$

and, employing the same procedures as for junction J_2, we eventually obtain

$$\begin{pmatrix} (\tilde{I}_n^{(re)}(L_{3,2},s))_{T_{3,2}} \\ (\tilde{I}_n^{(re)}(0,s))_{T_{3,4}} \end{pmatrix} = \begin{pmatrix} (\zeta_{n,m})_{10} & (\zeta_{n,m})_{11} \\ (\zeta_{n,m})_{12} & (\zeta_{n,m})_{13} \end{pmatrix} \begin{pmatrix} (\tilde{I}_n^{(i)}(L_{3,2},s))_{T_{3,2}} \\ (\tilde{I}_n^{(i)}(0,s))_{T_{3,4}} \end{pmatrix}$$

For junction J_4,

$$(C_{I_{n,m}})_{J_4} = \left[\begin{array}{c|cc} \text{Tube } T_{4,3} & \multicolumn{2}{c}{\text{Tube } T_{4,2}} \\ \hline 0 & 1 & 1 \\ 1 & 0 & 0 \end{array}\right]$$

and

$$\begin{pmatrix} (\tilde{I}_n^{(re)}(L_{4,3},s))_{T_{4,3}} \\ (\tilde{I}_n^{(re)}(L_{4,2},s))_{T_{4,2}} \end{pmatrix} = \begin{pmatrix} (\zeta_{n,m})_{14} & (\zeta_{n,m})_{15} \\ (\zeta_{n,m})_{16} & (\zeta_{n,m})_{17} \end{pmatrix} \cdot \begin{pmatrix} (\tilde{I}_n^{(i)}(L_{4,3},s))_{T_{4,3}} \\ (\tilde{I}_n^{(i)}(L_{4,2},s))_{T_{4,2}} \end{pmatrix}$$

The network scattering matrix $(\tilde{S}_{n,m}(s))_N$ is obtained by suitably rearranging the above junction scattering matrices so that the ordering of the components of the incident and reflected currents is the same as in the propagation equation. Thus, this equation becomes

$$
\begin{bmatrix}
(\tilde{I}_n^{(re}(0,s))_{T_{1,2}} \\
(\tilde{I}_n^{(re)}(L_{2,1},s))_{T_{2,1}} \\
(\tilde{I}_n^{(re)}(0,s))_{T_{2,3}} \\
(\tilde{I}_n^{(re)}(L_{3,2},s))_{T_{3,2}} \\
(\tilde{I}_n^{(re)}(0,s))_{T_{2,4}} \\
(\tilde{I}_n^{(re)}(L_{4,2},s))_{T_{4,2}} \\
(\tilde{I}_n^{(re)}(0,s))_{T_{3,4}} \\
(\tilde{I}_n^{(re)}(L_{4,3},s))_{T_{4,3}}
\end{bmatrix}
=
\begin{bmatrix}
(S_{n,m})_{J_1} & (0_{n,m}) & (0_{n,m}) & (0_{n,m}) & (0_{n,m}) & (0_{n,m}) & (0_{n,m}) & (0_{n,m}) \\
(0_{n,m}) & (\zeta_{n,m})_1 & (\zeta_{n,m})_2 & (0_{n,m}) & (\zeta_{n,m})_3 & (0_{n,m}) & (0_{n,m}) & (0_{n,m}) \\
(0_{n,m}) & (\zeta_{n,m})_4 & (\zeta_{n,m})_5 & (0_{n,m}) & (\zeta_{n,m})_6 & (0_{n,m}) & (0_{n,m}) & (0_{n,m}) \\
(0_{n,m}) & (0_{n,m}) & (0_{n,m}) & (\zeta_{n,m})_{10} & (0_{n,m}) & (0_{n,m}) & (\zeta_{n,m})_{11} & (0_{n,m}) \\
(0_{n,m}) & (\zeta_{n,m})_7 & (\zeta_{n,m})_8 & (0_{n,m}) & (\zeta_{n,m})_9 & (0_{n,m}) & (0_{n,m}) & (0_{n,m}) \\
(0_{n,m}) & (0_{n,m}) & (0_{n,m}) & (0_{n,m}) & (0_{n,m}) & (\zeta_{n,m})_{17} & (0_{n,m}) & (\zeta_{n,m})_{16} \\
(0_{n,m}) & (0_{n,m}) & (0_{n,m}) & (\zeta_{n,m})_{12} & (0_{n,m}) & (0_{n,m}) & (\zeta_{n,m})_{13} & (0_{n,m}) \\
(0_{n,m}) & (0_{n,m}) & (0_{n,m}) & (0_{n,m}) & (0_{n,m}) & (\zeta_{n,m})_{15} & (0_{n,m}) & (0_{n,m})_{14}
\end{bmatrix}
\begin{bmatrix}
(\tilde{I}_n^{(i)}(0,s))_{T_{1,2}} \\
(\tilde{I}_n^{(i)}(L_{2,1},s))_{T_{2,1}} \\
(\tilde{I}_n^{(i)}(0,s))_{T_{2,3}} \\
(\tilde{I}_n^{(i)}(L_{3,2},s))T_{3,2} \\
(\tilde{I}_n^{(i)}(0,s))_{T_{2,4}} \\
(\tilde{I}_n^{(i)}(L_{4,2},s))_{T_{4,2}} \\
(\tilde{I}_n^{(i)}(0,s))_{T_{3,4}} \\
(\tilde{I}_n^{(i)}(L_{4,3},s))_{T_{4,3}}
\end{bmatrix}
\tag{24}
$$

Equations (23) and (24) contain all the matrices required to solve the BLT equation.

2. Numerical Examples

A general computer code, QV7T, has been developed for treating this class of transmission-line problems. Both time harmonic and transient results are obtained, the latter being provided by a FFT algorithm (ref. 25).

To demonstrate that the above approach can solve transmission-line problems involving closed loops, a simple example involving only single transmission lines is first presented. The use of single-line configuration avoids unnecessary complications inherent in the multi-conductor analysis and serves to illustrate typical results. Results for a multiconductor network will then be illustrated.

For the single-wire example, Figure 4 shows a simple five-junction, five-tube network, which contains a single loop and is excited by a voltage source. The characteristic impedances of each line are $75\,\Omega$, the propagation velocities are all 3×10^8 meters/sec and all lengths are 1 meter. All junctions with the exception of junction J_5 have zero intrinsic impedances, so that the current scattering matrix for these junctions depend only on the number and impedances of lines connecting the particular junction. Junction J_5 is assumed matched with a $75\,\Omega$ load. A single voltage source in the transmission line connecting junctions J_1 and J_2 provides the excitation for the network. This source is located midway between the junctions at $z = .5$ meters, and is denoted by V_S.

Figure 5 shows the magnitude of the voltage at the $75\,\Omega$ load, denoted by V_L, at junction J_5, as a function of frequency for a unit voltage excitation. The various peaks observed in this spectrum are due to resonances within the loop structure, as well as resonances on the transmission line connecting junctions J_3 and J_5.

---

25. Cooley, J.W., and J.W. Tukey, "An Algorithm for the Machine Computation of Complex Fourier Series," Math. Comput., Vol. 19, 297-301, April 1965.

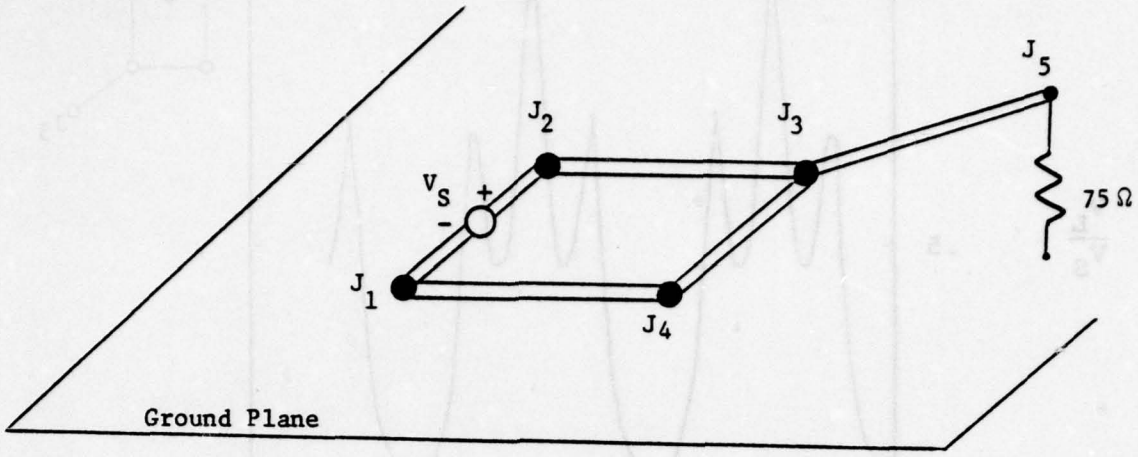

(a)

Line lengths = 1 meter
Line impedances = 75 Ω
Propagation Velocities = 3×10^8 m/sec

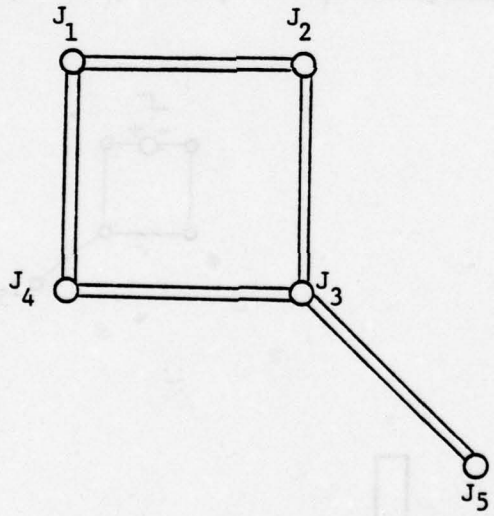

(b)

Figure 4. (a) Physical configuration of single-wire transmission-line network.

(b) Connected graph for transmission-line network.

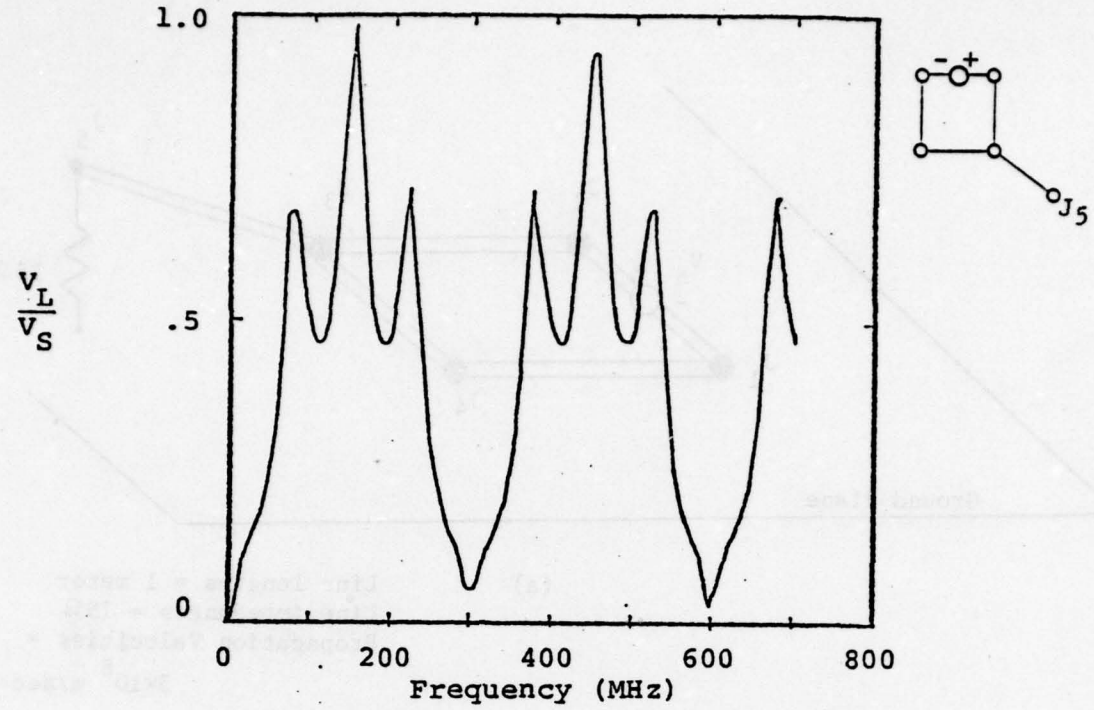

Figure 5. Impulse spectrum of load voltage at junction J_5.

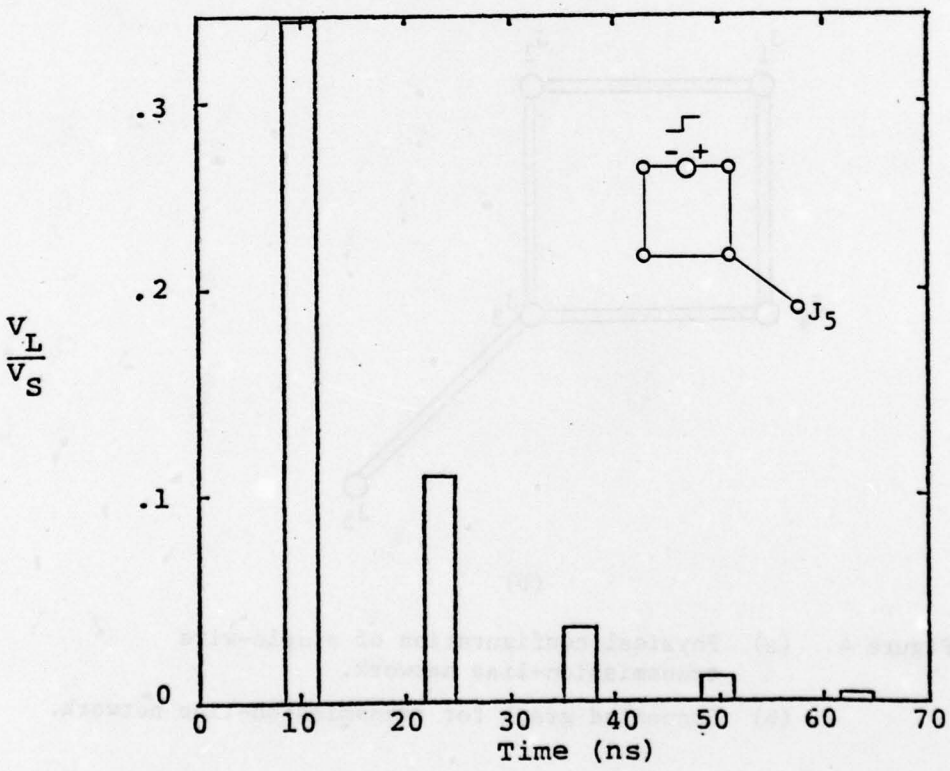

Figure 6. Step function excited load voltage at junction J_5.

By multiplying this impulse response spectrum by the spectrum of a step function voltage and performing a numerical Fourier transformation, the step function response at the load can be determined. This is illustrated in Figure 6. Note that even though the circulating loop current goes to infinity as time progresses, the load voltage (and hence load current) goes to zero, as required by a dc analysis. A careful examination of the times of arrival of the various voltage pulses provide one way of validating the correctness of the analysis.

Figure 7 shows the step excited load voltage at junction J_5 for the same network, but with the voltage source located in the mid-point of the transmission line connecting junctions J_3 and J_5. As in the previous case, the times of arrival between the various waves which comprise the total transient waveform shown in this figure can be used to verify the accuracy of the calculation. It should be noted that because there is no direct current connection from junction J_1, J_2, J_3, and J_4 to ground, the voltage of junction J_5 excited by a step function excitation V_S, will approach zero in late time, due to the lack of current flow through the 75Ω load at the junction J_5. The finite slope of the vertical lines of the waveform, most evident for late times, is caused by the fact that the transient waveform is sampled at discrete points. In the ideal case, these lines should have an infinite slope.

The transient response of the load voltage due to the two sources previously considered exciting the transmission line at the saem time is illustrated in Figure 8. Although this result is calculated directly using the BLT equation, the same result can be obtained by superimposing the results of Figures 6 and 7.

As an example of the results for a more complex multiconductor network, consider the transmission-line configuration, illustrated in Figure 9. As is indicated in that figure, the network consists of four transmission-line tubes. Tube $T_{1,2}$ is a three-wire transmission line with tubes $T_{2,3}$ and $T_{2,4}$ being two-wire lines. This is the same network as in Figure 1, but with different sources. The points at which the network

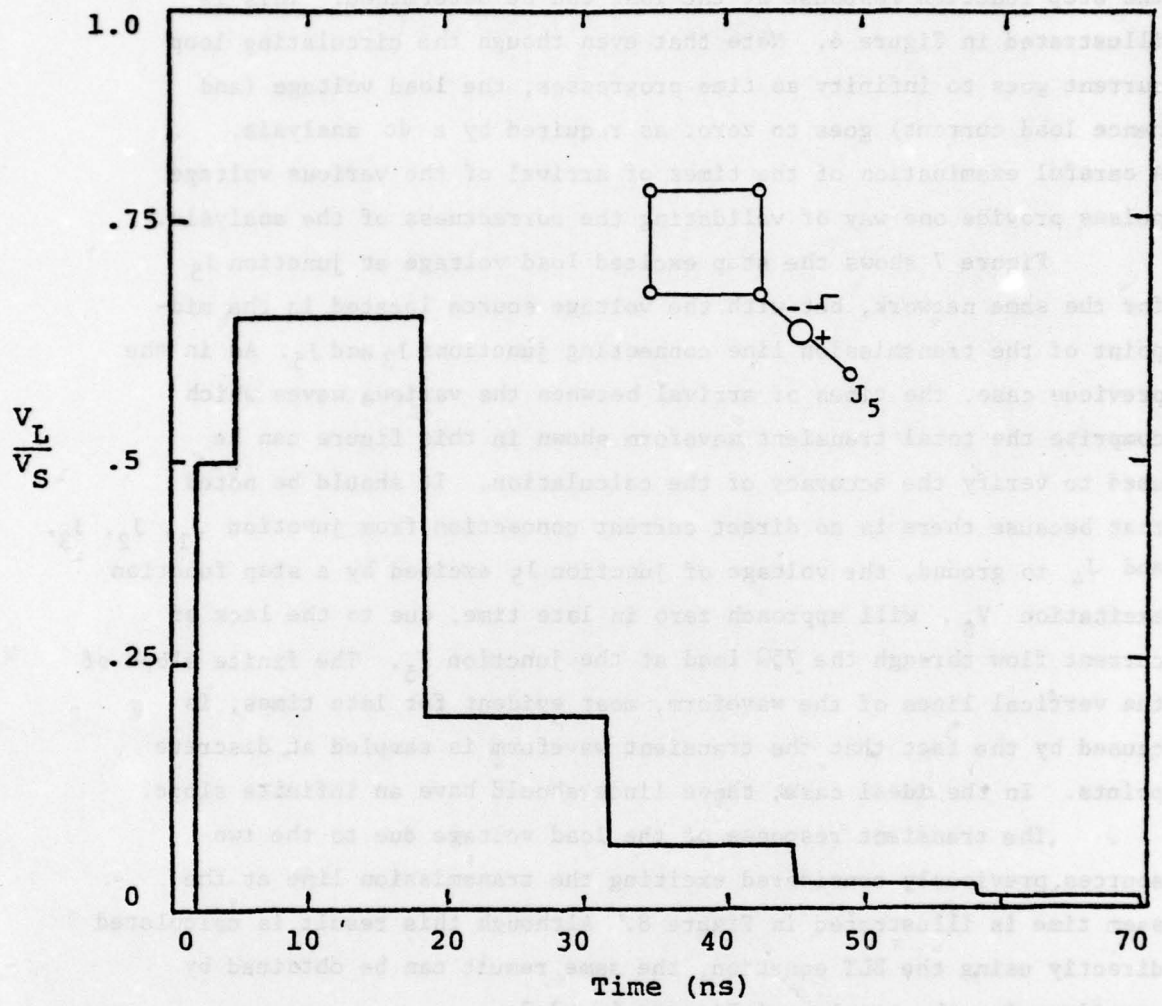

Figure 7. Step excited load voltage at junction J_5.

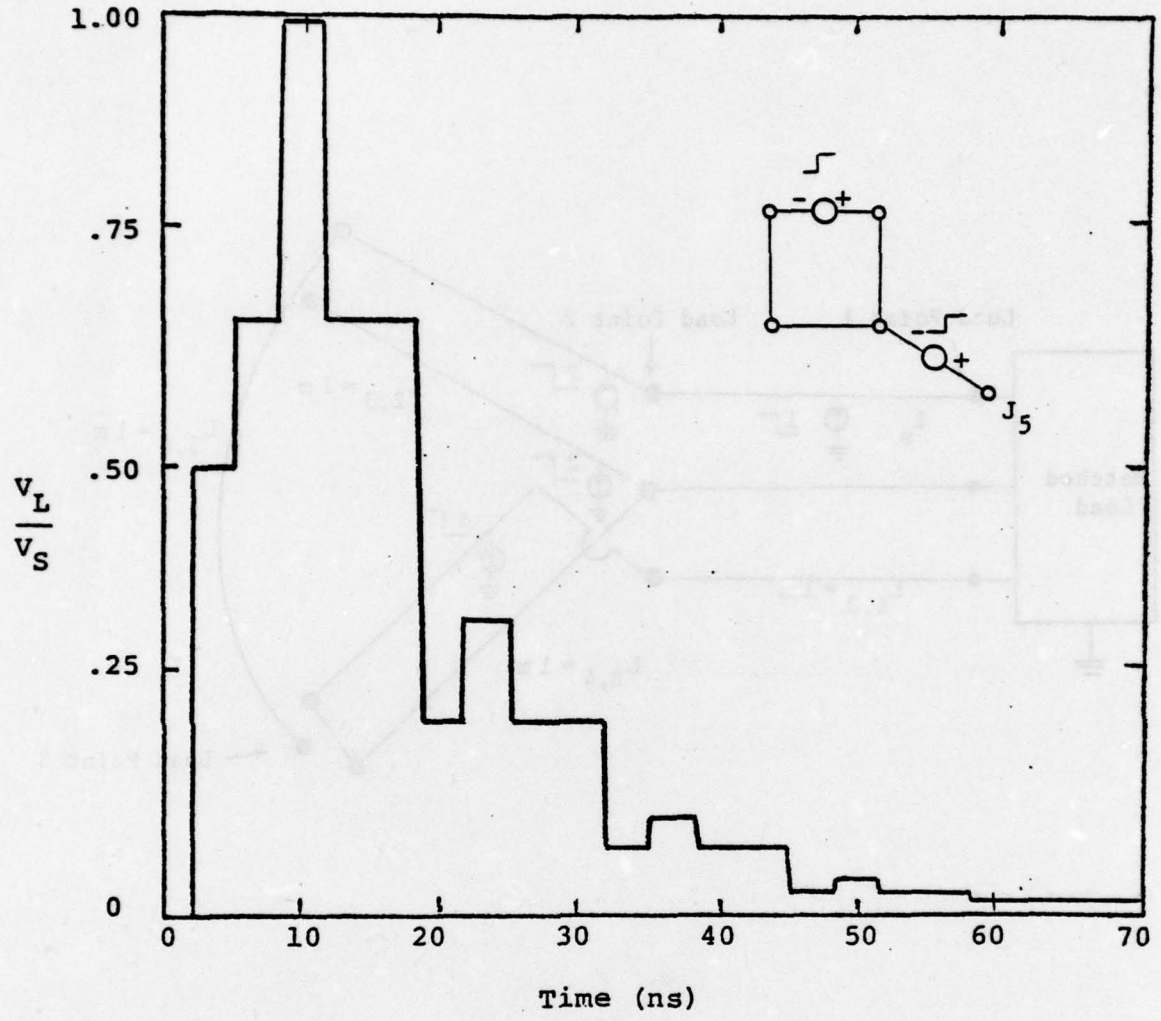

Figure 8. Step excited voltage at junction J_5 for two driving voltage sources, both of magnitude V_S.

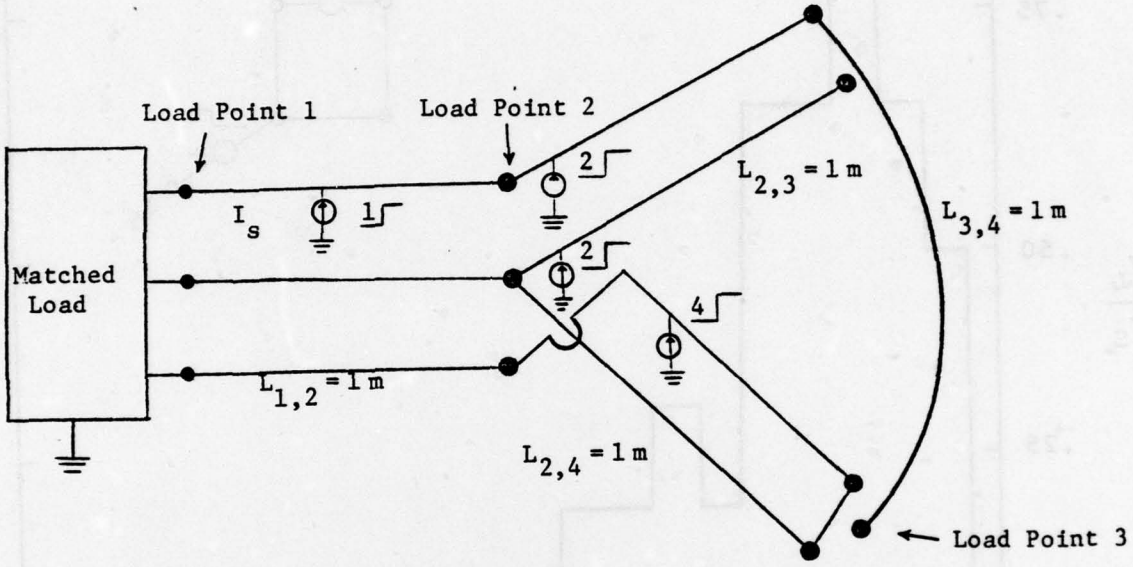

Figure 9. A simple multiconductor network with current sources.

response is calculated are also indicated. The linear graph for this network is the same as in Figure 1b.

For this example, each multiconductor tube length is assumed to be 1 meter long. For each tube, the capacitive coefficients were taken to be 6.0×10^{-11} farad/meter for the self (diagonal) terms and -1.0×10^{-11} farad/meter for the mutual (off diagonal) terms. The capacitive coefficient matrices for each line were assumed to be highly symmetric such that these two numbers completely describe the matrix. All propagation velocities on the multiconductor lines were assumed to be uniform and equal to 3.0×10^{8} m/s so that the inductance matrix is related to the inverse of the capacitive coefficient matrix.

For the single-wire transmission line in tube $T_{3,4}$, the characteristic line impedance was taken to be 100 ohms. That impedance, together with the assumed propagation speed of 3.0×10^{8} m/s determines the capacitance per unit length of that line.

The terminating impedance network at junction J_1 is chosen such that the line is perfectly matched. With the capacitive coefficient chosen as above, this matched load is described by an impedance matrix with the values 59.52 ohms on the diagonal and 11.90 ohms off the diagonal. Other terminations for the transmission-line tubes are indicated in Figure 9. Note that tube $T_{2,4}$ has its open circuit at junction J_4. Similarly, the second wire of tube $T_{2,3}$ is open circuited at junction J_3.

In this example, the sources exciting the transmission-line network are taken to be current sources. A step-function current source of magnitude I_s is applied at time $t = 0$ to the midpoint of the first wire in tube 1. Similarly, there are two current sources of magnitude $2I_s$ applied across tube $T_{2,3}$ at a distance of .1 meter from junction 2. Finally, tube $T_{2,4}$ is excited by a step function of magnitude $4I_s$ occurring at time $t = 0$. This current source is located at a distance .4 meter from junction J_2 and excites only the second wire of tube $T_{2,4}$.

For this example, the voltage response at three load points is considered. These load points are illustrated in Figure 9.

Figure 10 illustrates the step function, current-excited voltage across load point 1 as a function of time. This quanitity is normalized with respect to the quantity I_s. Note that due to the complexity of the transmission-line network, this response is much more complicated than responses previously seen.

The first contribution to the load voltage that arrives is due to a traveling wave from the source on tube $T_{1,2}$ to the load point .5 meter away. This corresponds to a time of 1.66 nanoseconds. The second arrival of a wave to load point 2 occurs from the sources on tube $T_{2,3}$ which are 1.1 meters away. This corresponds to a time of 3.66 nanoseconds.

The next arrival of a wave which contributes markedly to the voltage response at load point 1 is at 9.66 nanoseconds. This contribution arises from a wave traveling along the first wire of tube $T_{2,3}$ toward junction J_3. At junction J_3 there is a change of impedance level of the line, and a fraction of the wave is reflected, eventually returning to load point 1. The portion of the wave that is transmitted through junction J_3 continues along tube $T_{3,4}$ and suffers complete reflection at load 4, wehre there is an open-circuit condition. This wave eventually reflects back and reaches load point 1 at a time of $t = 16.33$ nanoseconds.

All of these times may be verified as being correct from the voltage plots presented in Figure 10. Each of the additional break points in the voltage plots of Figure 10 can be attributed to arrival times of various components of traveling waves on this transmission-line network.

Figure 11 illustrates similar results for the voltage at load point 2. Notice that the first time of arrival is at $t = .33$ nanoseconds which corresponds to the distance of .1 meter.

Figure 12 illustrates the step-function current-excited voltage response at load 3. The calculated turn-on time for this case is $t = 6.33$ nanoseconds and agrees well with the results of Figure 12. An additional check for this case is to investigate the behavior of the current at load point 3. Since this point is open circuit, it

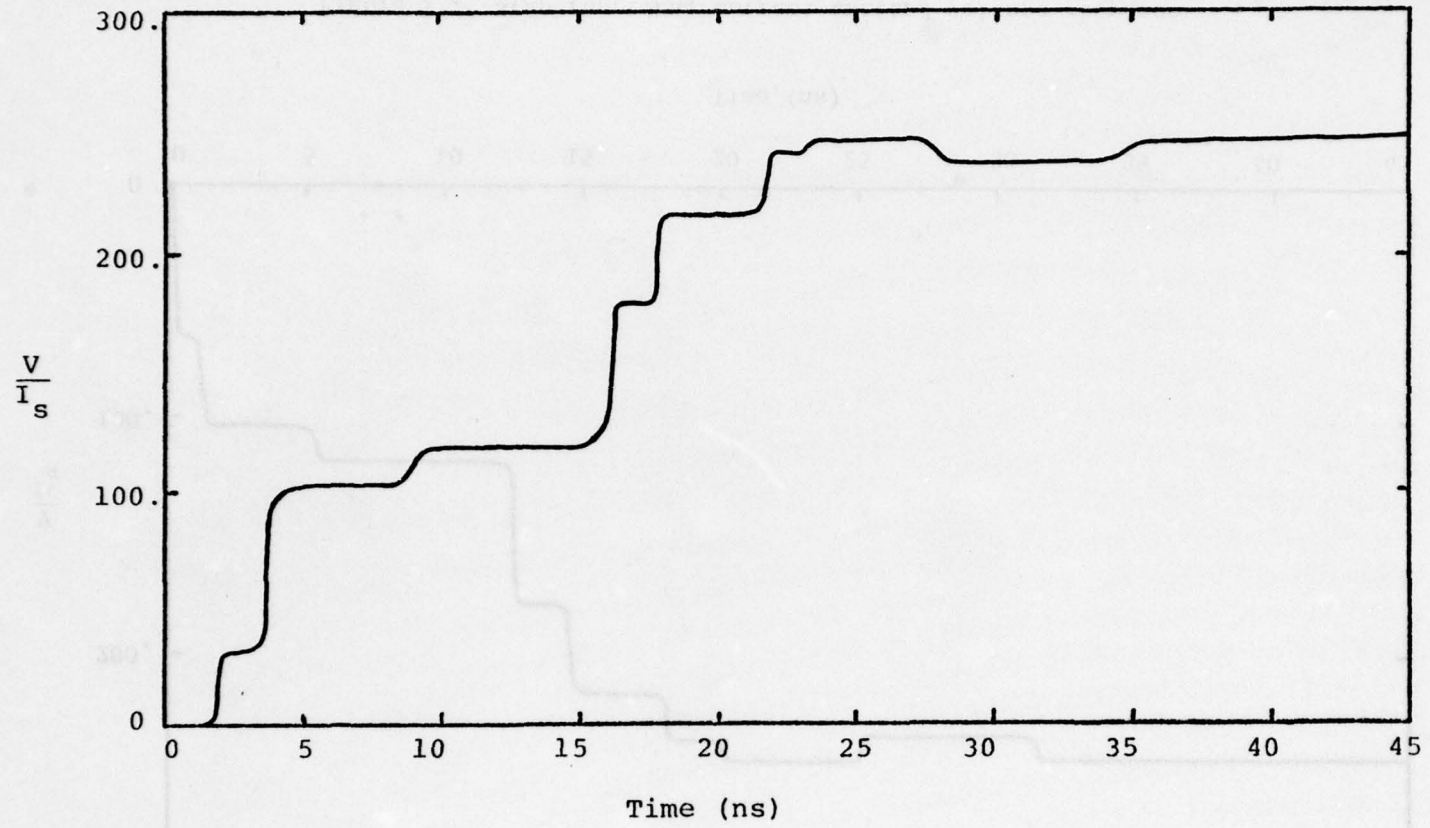

Figure 10. Step function, current-excited voltage response of network in Figure 9 at load point 1.

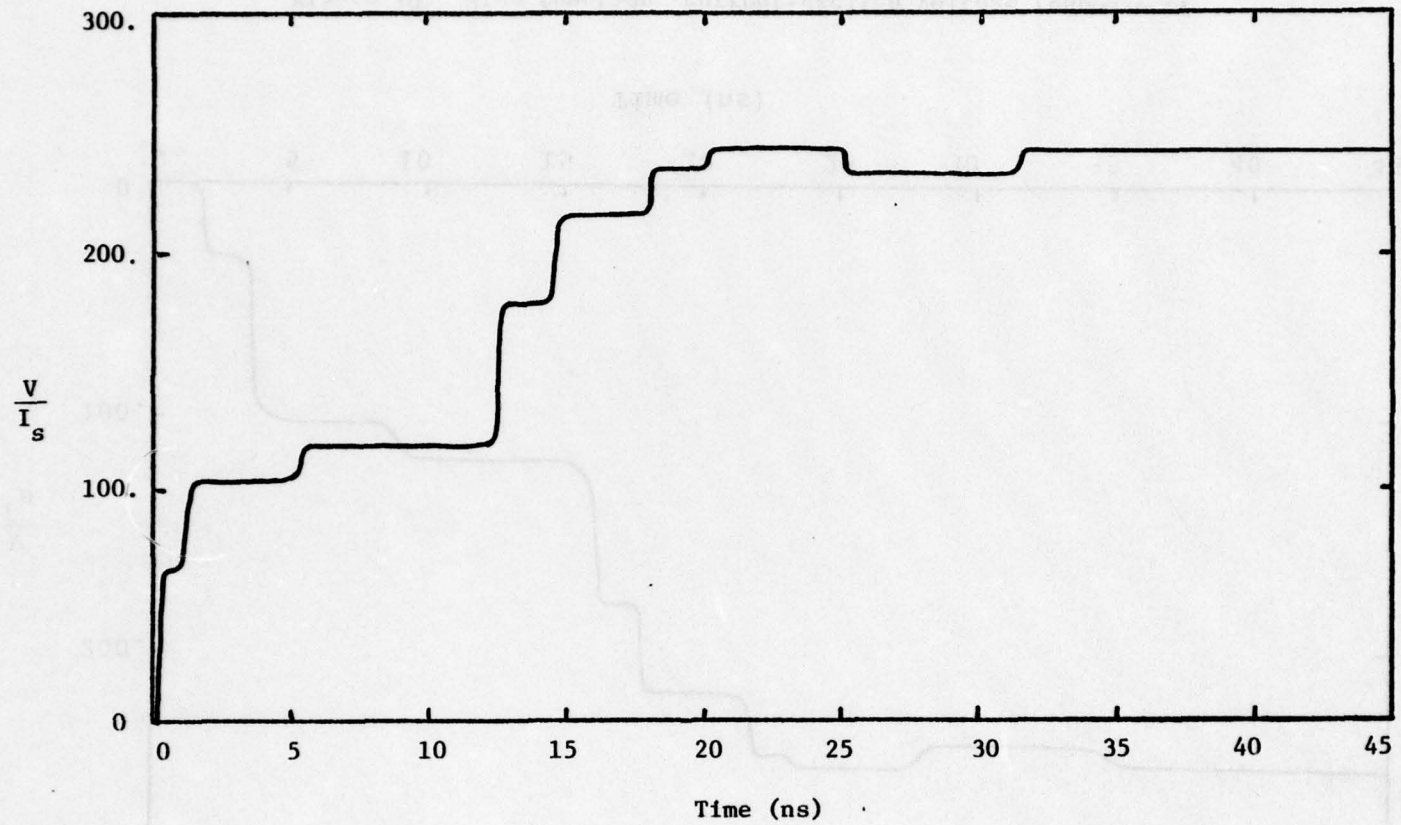

Figure 11. Step function, current-excited voltage response of network in Figure 9 at load point 2.

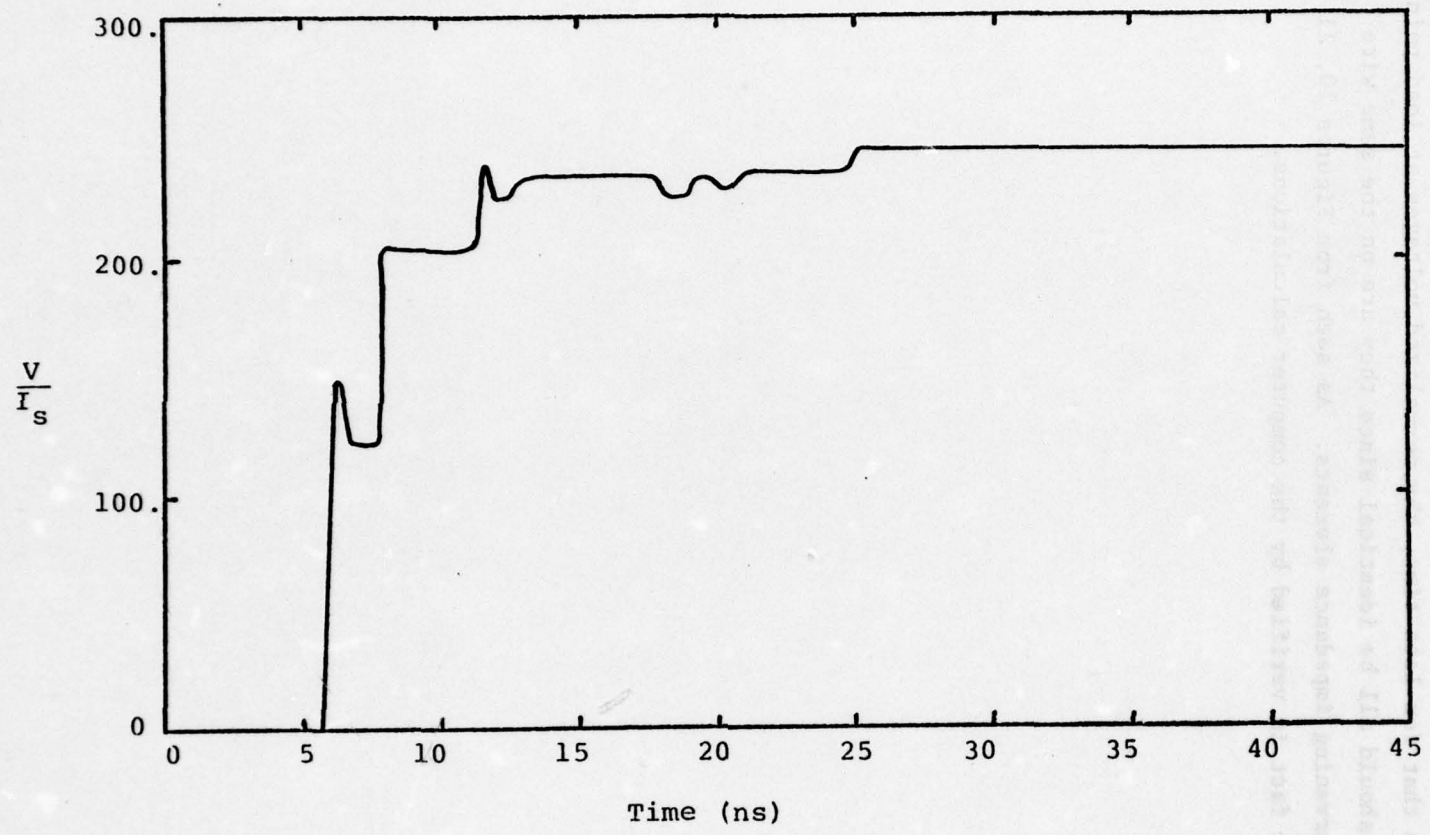

Figure 12. Step function, current-excited voltage response of network in Figure 9 at load point 3.

is required that the current be zero at this junction. This indeed was found to be the case.

Note that for late time, the normalized voltages at load points 1, 2, and 3 should all be identical since they are on the same wire with no intervening impedance elements. As seen from Figures 10, 11 and 12, this fact is verified by the computer calculations.

SECTION IV
CONCLUSION

This report has described and illustrated a technique for analyzing lossless, multiconductor transmission-line networks. This method solves for currents at all nodes at the same time, as opposed to solving the problem in a junction-by-junction manner as in the conventional method. The present approach has an added advantage of being able to treat transmission-line networks that contain one or more closed loops.

The ability to analyze tansmission-line networks with loops is important, especially for EMP applications where there is substantial energy in the low frequency portion of the spectrum. Current efforts involve extending this method so as to permit the analysis of general interconnections of multiconductor transmission lines which are excited not by lumped voltage and current sources, but by distributed sources which are provided by the incident EMP fields.

The analysis of a more general transmission-line network that may include losses will be reported in reference (24). This upcoming report also discusses in greater detail the general theory of transmission-line network analysis.

REFERENCES

1. Plonsey, R., and R.E. Collin, Principles and Applications of Electromagnetic Fields, McGraw Hill, 1961.

2. Tesche, F.M., et al., Evaluation of Present Internal EMP Interaction Technology: Description of Needed Improvements, AFWL-TR-75-288, Air Force Weapons Laboratory, Kirtland Air Force Base, NM, Oct. 1973.

3. Tesche, F.M., and T.K. Liu, Selected Topics in Transmission-Line Theory for EMP Internal Interaction Problems, AFWL-TR-77-73, Air Force Weapons Laboratory, Kirtland Air Force Base, NM, Dec. 1976.

4. Tesche, F.M., and T.K. Liu, An Electric Model for a Cable Clamp on a Single-Wire Transmission Line, AFWL-TR-76-325, Air Force Weapons Laboratory, Kirtland Air Force Base, NM, Mar. 1977.

5. Coen, S., T.K. Liu, and F.M. Tesche, Calculation of the Equivalent Capacitance of a Rib near a Single-Wire Transmission Line, AFWL-TR-77-60, Air Force Weapons Laboratory, Kirtland Air Force Base, NM, June 1977.

6. Lee, K.S.H., and F.C. Yang, A Wire Passing by a Circular Aperture in an Infinite Ground Plane, AFWL-TR-77-52, Air Force Weapons Laboratory, Kirtland Air Force Base, NM, Feb. 1977.

7. Lam, J., Equivalent Lumped Parameters for a Bend in a Two-Wire Transmission Line, AFWL-TR-77-5, Air Force Weapons Laboratory, Kirtland Air Force Base, NM, Jan. 1977.

8. Lam, J., Propagation Characteristics of a Periodically Loaded Transmission Line, AFWL-TR-76-324, Air Force Weapons Laboratory, Kirtland Air Force Base, NM, Jan. 1977.

9. Liu, T.K., Electromagnetic Coupling between Multiconductor Transmission Lines in a Homogeneous Medium, AFWL-TR-76-333, Air Force Weapons Laboratory, Kirtland Air Force Base, NM, May 1977.

10. EMP Handbook for Missiles and Aircraft in Flight. Also, EMP Interaction 1-1.

11. Carson, J.R., "The Rigorous and Approximate Theories of Electrical Transmission along Wires," Bell System Technical Journal, No. 1, Jan. 1928, pp. 11-23.

12. Kuznetsov, P.I., and R.L. Stratonovich, The Propagation of Electromagnetic Waves in Multiconductor Transmission Lines, Pergamon Press, Oxford, England, 1964.

13. Kajfez, D., "Multiconductor Transmission Lines," AFWL EMP Interaction Notes, Note 151, June 1972.

14. Paul, C.R., "On Uniform Multimode Transmission Lines," IEEE Trans. M.T.T., Vol. MTT-21, No. 8, Aug. 1973, pp. 556-558.

15. Paul, C.R., "Efficient Numerical Computation of the Frequency Response of Cables Illuminated by an Electromagnetic Field," IEEE Trans. M.T.T., Vol. MTT-52, No. 4, Apr. 1974, pp. 454-457.

16. Paul, C.R., "Useful Matrix Chain Parameter Identities for the Analysis of Multiconductor Transmission Lines," IEEE Trans. M.T.T., Spet. 1975, pp. 756-760.

17. Frankel, S., Cable and Multiconductor Transmission Analysis, Harry Diamond Laboratory, HDL-TR-091-1, June 1974.

18. Lenahan, T.A., "The Theory of Uniform Cables, Parts I & II," Bell System Technical Journal, April 1977, pp. 597-625.

19. Collin, R.E., Foundations for Microwave Engineering, McGraw Hill, New York, 1966.

20. Desoer, C.A., and E.S.Kuh, Basic Circuit Theory, McGraw Hill, New York, 1969.

21. Baum, C.E., "The Role of Scattering Theory in Electromagnetic Interference Problems," in Electromagnetic Scattering, P.L.E. Uslenghi (ed.), to be published.

22. Baum, C.E., "Coupling into Coaxial Cables from Currents and Charges on the Exterior," presented at the 1976 URSI Meeting, Amherst, Mass.

23. Tesche, F.M., "A General Multiconductor Transmission-Line Model," presented at the 1976 URSI Meeting, Amherst, Mass.

24. Baum, C.E., T.K. Liu and F.M. Tesche, "On the General Analysis of Multiconductor Transmission-Line Networks," AFWL EMP Interaction Notes, to be published.

25. Cooley, J.W., and J.W. Tukey, "An Algorithm for the Machine Computation of Complex Fourier Series," Math. Comput. Vol. 19, 297-301, April 1965.